The Absence of uPAR Is Associated with the Progression of Dermal Fibrosis

Yosuke Kanno[1], Aki Kaneiwa[1], Misato Minamida[1], Miho Kanno[1], Kanji Tomogane[1,2], Koji Takeuchi[2], Kiyotaka Okada[3], Shigeru Ueshima[3], Osamu Matsuo[3] and Hiroyuki Matsuno[1]

The fibrinolytic system is considered to play an important role in the degradation of extracellular matrices (ECM). However, the detailed mechanism regarding how this system affects fibrosis remains unclear. Urokinase-type plasminogen activator receptor (uPAR) not only functions as a proteinase receptor but also plays a role in cellular adhesion, differentiation, proliferation, and migration through intracellular signaling. To investigate the effect of uPAR on dermal fibrosis, the skin of wild-type mice was compared with uPAR-deficient ($uPAR^{-/-}$) mice. The results showed that the absence of uPAR increases dermal thickness. In addition, collagen synthesis as well as the number of myofibroblasts was greater in the skin of $uPAR^{-/-}$ mice than in the skin of $uPAR^{+/+}$ mice. Moreover, we showed that the absence of uPAR attenuates the activity of matrix metalloproteinases (MMP)-2, 9 in the skin. In conclusion, this study suggests that the absence of uPAR not only regulates fibrosis-related gene expression and MMP activity but also results in ECM deposition. Therefore, the absence of uPAR induces dermal fibrosis. These findings provide new insights into the role of uPAR on dermal fibrosis.

Journal of Investigative Dermatology (2008) **128,** 2792–2797; doi:10.1038/jid.2008.157; published online 12 June 2008

INTRODUCTION

Systemic sclerosis (SSc; scleroderma) is characterized by excessive fibrosis of the skin and internal organs due to excessive accumulation of extracellular matrix (ECM). The mechanisms resulting in fibrosis in SSc are still unknown. Fibrotic changes lead to destruction of normal histologic structures in the skin and other organs. There are still no effective treatments to prevent or halt the progression of fibrosis in SSc and other fibrotic diseases (Highland and Silver, 2005).

The fibrinolytic system contains plasminogen, a proenzyme, that is converted into the active serine protease plasmin, a main component of the fibrinolytic system, through the action of a tissue-type plasminogen activator or urokinase-type PA (uPA)/uPA receptor (uPAR). The fibrinolytic system is considered to play an important role in the degradation of extracellular matrices (ECM). However, the detailed mechanism of how this system affects fibrosis remains unclear.

uPAR is a glycosylated 50–60 kDa protein that concentrates serin protease activity in the pericellular region (Mondino *et al.*, 1999). Recent studies indicate that uPAR not only functions in cell surface uPA activity and plasmin generation but also plays a role in cellular adhesion, differentiation, proliferation, and migration through intracellular signaling (Blasi and Carmeliet, 2002). Moreover, uPAR involves in SSc and other fibrotic diseases (Zhang *et al.*, 2003; D'Alessio *et al.*, 2004; Margheri *et al.*, 2006).

This study was performed to assess the role of uPAR in the development of dermal fibrosis. We herein report, for the first time, the crucial role of uPAR on dermal fibrosis.

RESULTS

The dermal surface features in $uPAR^{+/+}$ mice and $uPAR^{-/-}$ mice

The skin distension ability of $uPAR^{+/+}$ mice was compared to that of $uPAR^{-/-}$ mice. The skin distension ability of $uPAR^{+/+}$ mice was 1.28-fold greater than that of $uPAR^{-/-}$ mice at the age of 18 weeks (Figure 1a). However, there was no difference between $uPAR^{+/+}$ mice and $uPAR^{-/-}$ mice at the age of 6 and 10 weeks. In addition, there was no difference between the male and female mice (data not shown). Moreover, to investigate the effect of uPAR deficiency in the skin, the dermal surface features of $uPAR^{+/+}$ mice and $uPAR^{-/-}$ mice were observed using electron microscopy (Figure 1b). The wrinkles on the skin of $uPAR^{-/-}$ mice decreased by the progression of dermal fibrosis.

[1]*Department of Clinical Pathological Biochemistry, Faculty of Pharmaceutical Science, Doshisha Women's Collage of Liberal Arts, Kyoto, Japan;* [2]*Department of Pharmacology and Experimental Therapeutics, Kyoto Pharmaceutical University, Misasagi, Yamashina, Kyoto, Japan and* [3]*Department of Physiology II, Kinki University School of Medicine, Osaka-sayama, Japan*

Correspondence: Dr Yosuke Kanno, Department of Clinical Pathological Biochemistry, Faculty of Pharmaceutical Science, Doshisha Women's Collage of Liberal Arts, 97-1 Kodo, Kyo-tanabe 610-0395 Kyoto, Japan. E-mail: ykanno@dwc.doshisha.ac.jp

Abbreviations: ECM, extracellular matrix; MMP, matrix metalloproteinase; PAI-1, plasminogen activator inhibitor-1; RT-PCR, reverse transcription-PCR; α-SMA, α-smooth muscle actin; SSc, systemic sclerosis; uPAR, urokinase-type plasminogen activator receptor; $uPAR^{-/-}$, uPAR-deficient mice

Received 26 November 2007; accepted 23 April 2008; published online 12 June 2008

The skin histology in uPAR$^{+/+}$ mice and uPAR$^{-/-}$ mice

A histological examination of the skin demonstrated a considerable increase in the dermal thickness of uPAR$^{-/-}$ mice as compared with uPAR$^{+/+}$ mice (Figure 2a). A quantitative analysis showed the dermal thickness of uPAR$^{-/-}$ mice to be 1.25-fold greater than that of uPAR$^{+/+}$ mice (Figure 2b). Masson's trichrome staining revealed an accumulation of ECM components. Figure 2c shows that the accumulation of ECM components was greater in the skin of uPAR$^{-/-}$ mice than in that of uPAR$^{+/+}$ mice. These data suggest that the absence of uPAR induces the development of dermal fibrosis.

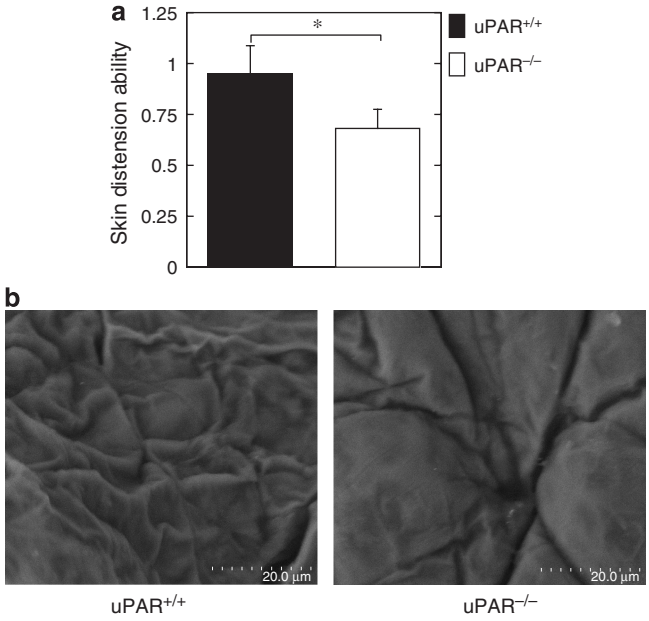

Figure 1. The dermal surface features in uPAR$^{+/+}$ mice and uPAR$^{-/-}$ mice. (**a**) Skin distension ability of uPAR$^{+/+}$ mice and uPAR$^{-/-}$ mice at the age of 18 weeks ($n=6$). Skin distension ability was measured as described in the Materials and Methods section. The data represent the mean ± SEM. *$P<0.05$. (**b**) Electron microscopy of dermis in the skin of uPAR$^{+/+}$ mice and uPAR$^{-/-}$ mice at the age of 18 weeks.

The expression of uPAR in the skin

The expression of uPAR was examined by reverse transcription-PCR (RT-PCR), western blot analysis, and immunohistochemistry in the skin of wild-type mice at the age of 6, 10, and 18 weeks (Figure 3a–d). The expression of uPAR in the skin of wild-type mice increased with advancing age.

The effect of uPAR deficiency on dermal ECM deposition

To investigate the effect of uPAR deficiency on dermal collagen deposition, the collagen content in the skin of uPAR$^{+/+}$ mice and uPAR$^{-/-}$ mice was measured using Sirius red staining (Figure 4a). The collagen content in the skin of uPAR$^{-/-}$ mice was 1.82-fold greater than that in the skin of uPAR$^{+/+}$ mice. An increased accumulation of myofibroblasts in the dermis, which is characteristic of scleroderma, is believed to contribute to the pathogenesis. To compare the accumulation of myofibroblasts in the skin of uPAR$^{+/+}$ mice and uPAR$^{-/-}$ mice, the expression of α-smooth muscle actin (α-SMA) was examined. The number of α-SMA-positive cells was 3.34-fold greater in the skin of uPAR$^{-/-}$ mice than that in the skin of uPAR$^{+/+}$ mice (Figure 4b and c). The expression of fibrosis-related genes, type I collagen, type IV collagen, plasminogen activator inhibitor (PAI)-1, matrix metalloproteinases (MMP)-2 and MMP-9 were examined by RT-PCR analysis (Figure 4d). The expression of type I collagen, type IV collagen, and PAI-1 was greater in uPAR$^{-/-}$ mice than that in uPAR$^{+/+}$ mice. On the other hand, the expression of MMP-2 and MMP-9 in uPAR$^{-/-}$ mice was less than that in uPAR$^{+/+}$

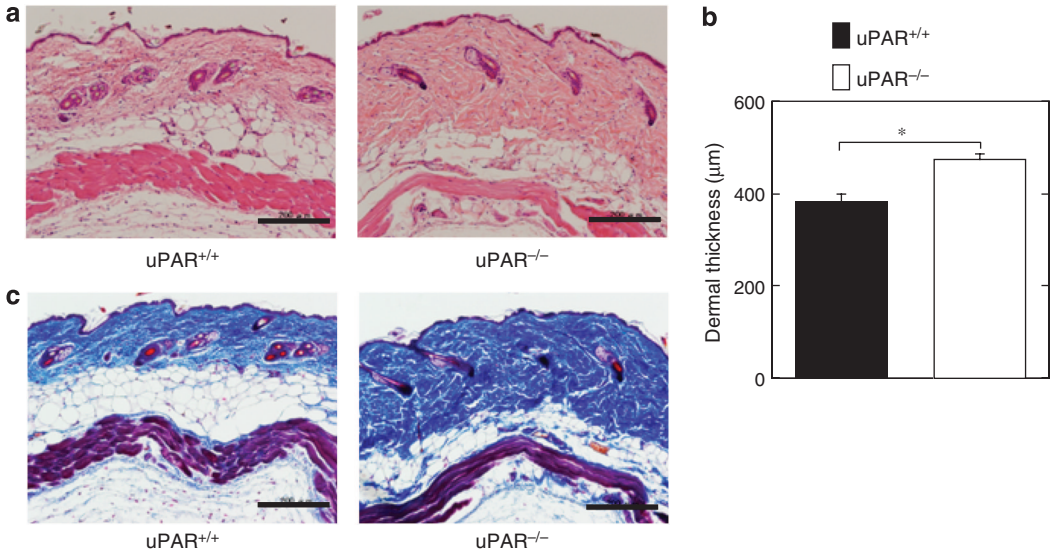

Figure 2. The skin histology in uPAR$^{+/+}$ mice and uPAR$^{-/-}$ mice. (**a**) Paraffin-embedded sections of uPAR$^{+/+}$ mice and uPAR$^{-/-}$ mice at the age of 18 weeks were stained with hematoxylin and eosin. Scale bar = 200 μm. (**b**) The dermal thickness (distance from the epidermal–dermal junction to dermal–muscle junction) was measured in skin sections from uPAR$^{+/+}$ mice and uPAR$^{-/-}$ mice at the age of 18 weeks ($n=7$). The data represent the mean ± SEM. *$P<0.01$. (**c**) Paraffin-embedded sections of uPAR$^{+/+}$ mice and uPAR$^{-/-}$ mice at the age of 18 weeks were stained with Masson's trichrome stain. Scale bar = 200 μm.

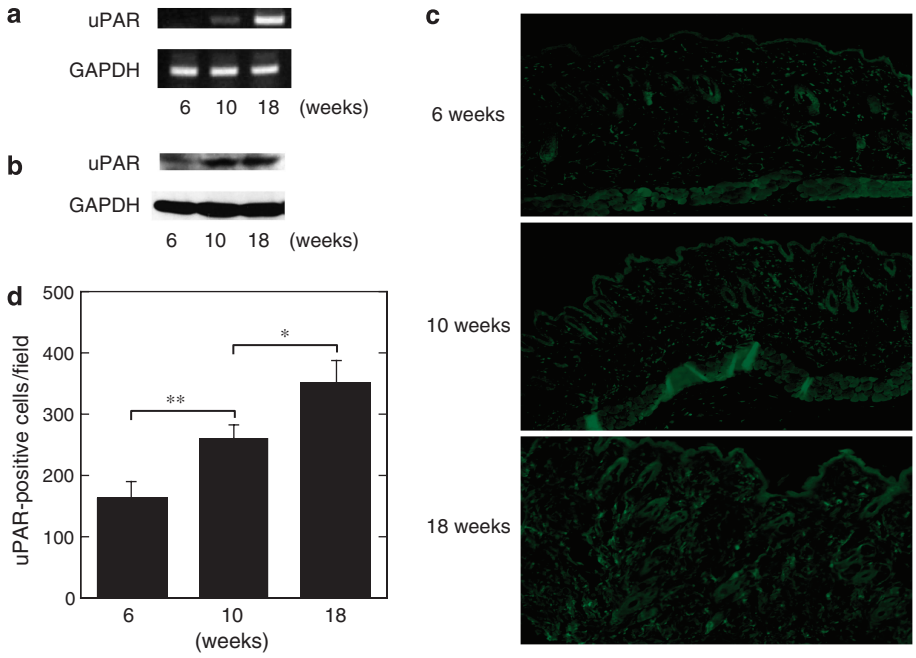

Figure 3. The expression of uPAR in the skin of wild-type mice. (**a**) uPAR gene expression in the skin of wild-type mice at the age of 6, 10, and 18 weeks was determined by RT-PCR. (**b**) The expression of uPAR in skin of wild-type mice at the age of 6, 10, and 18weeks was determined by a western blot analysis. Similar results were obtained with three additional and different skin samples. (**c**) Immunohistochemistry for uPAR in the skin of wild-type mice at the age of 6, 10, and 18 weeks. Paraffin sections were stained with antibodies to uPAR as described in the Materials and Methods section. (**d**) The number of uPAR-positive cells on the skin of wildtype mice at the age of 6, 10, and 18weeks was determined at four randomly selected sites from different sections. The data represent the mean ± SEM. $*P<0.01$. $**P<0.05$.

mice. In addition, the absence of uPAR attenuates the activity of MMP-2 and MMP-9 (Figure 4e). The data suggest that the absence of uPAR induces the accumulation of ECM components.

DISCUSSION

This study demonstrated that the absence of uPAR develops the progression of dermal fibrosis.

The initial observations showed that the absence of uPAR decreased skin distension ability and increased dermal thickness. The dermal surface of $uPAR^{-/-}$ mice seems to be tighter than that of $uPAR^{+/+}$ mice. The absence of uPAR might play an important role in the development of dermal fibrosis.

The skin distension ability in $uPAR^{-/-}$ mice decreased as compared with the skin of $uPAR^{+/+}$ mice at the age of 18 weeks, although there was no difference between $uPAR^{+/+}$ mice and $uPAR^{-/-}$ mice at the age of 6 and 10 weeks. The expression of uPAR in the skin of wild-type mice at the age of 6, 10, and 18 weeks was analyzed to investigate whether the expression of uPAR was associated with aging in the skin. The expression of uPAR increased with advancing age. The hypothesis is that aging induced the expression of uPAR in skin, where uPAR acts in a negative feedback loop. These data suggest that the absence of uPAR might not be able to repress the age-related progression of dermal fibrosis.

Fibrosis is characterized by the excessive accumulation of ECM proteins (Knapp *et al.*, 1977; Hunt, 1990). In normal physiological tissue remodeling, a careful balance is maintained between collagen synthesis and degradation, culminating in a final collagen content that is similar, although not identical, to the original tissue (Parks, 1999). The current study shows that ECM deposition was greater in the skin of $uPAR^{-/-}$ mice than in that of $uPAR^{+/+}$ mice. In addition, the collagen content and the expression of type I collagen and type IV collagen was greater in the skin of $uPAR^{-/-}$ mice than that in $uPAR^{+/+}$ mice. The presence of myofibroblasts is consistent with the pathology of fibrotic diseases (Sappino *et al.*, 1990; Ludwicka *et al.*, 1992). Myofibroblasts are specialized cells with high synthetic capacity for ECM proteins (Gabbiani, 2003). The number of myofibroblasts was greater in the skin of $uPAR^{-/-}$ mice than in the skin of $uPAR^{+/+}$ mice. Bernstein *et al.* (2007) suggest that down-regulation of uPAR is necessary for myofibroblast differentiation. The absence of uPAR might induce myofibroblast differentiation. Moreover, the expression of PAI-1 was greater in the skin of $uPAR^{-/-}$ mice than that in $uPAR^{+/+}$ mice. Bleomycin-induced fibrosis is more severe in transgenic mice overexpressing PAI-1 and less so in PAI-1-deficient mice (Eitzman *et al.*, 1996). According to this alternative model, the elevated PAI-1 promotes collagen deposition not by inhibiting plasmin, but by stimulating the migration of leukocytes and collagen-producing cells into the damaged tissue (Loskutoff and Quigley, 2000). The protection from fibrosis by PAI-1 deficiency is dependent on increased proteolytic activity of the plasminogen activator system (Hattori *et al.*, 2000). The reduction of the plasmin activity due to a deficiency of uPAR, also in association with an

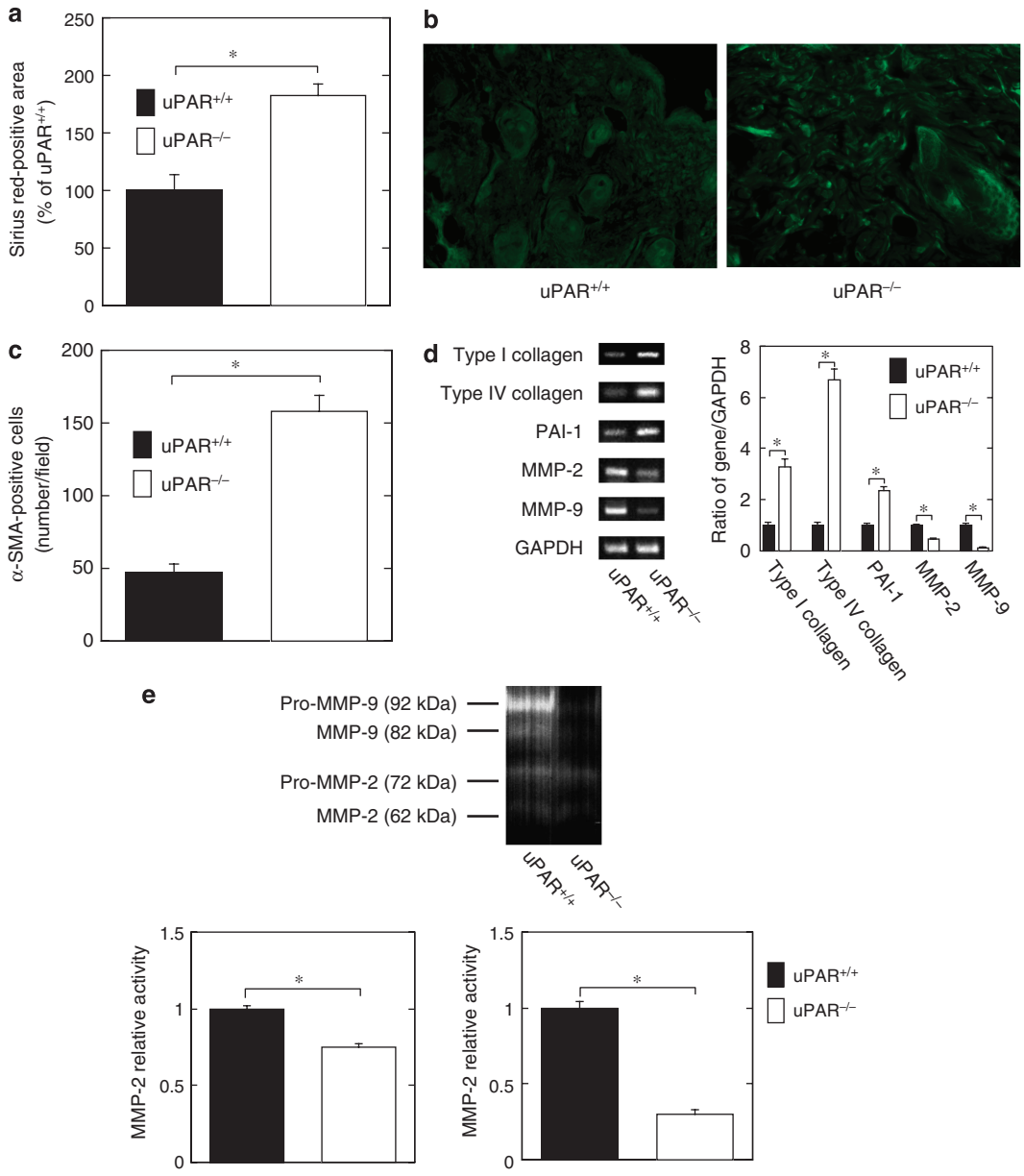

Figure 4. The effect of uPAR deficiency on dermal ECM deposition. (**a**) The collagen content was measured by a Sirius red stain on the skin of uPAR$^{+/+}$ mice and uPAR$^{-/-}$ mice at the age of 18 weeks ($n=5$). Sirius red-positive area was expressed as a percent of the observed in uPAR$^{+/+}$ mice. The data represent the mean ± SEM. *$P<0.01$. (**b**) Immunohistochemistry for α-smooth muscle actin (α-SMA)-positive cells on the skin of uPAR$^{+/+}$ mice and uPAR$^{-/-}$ mice at the age of 18 weeks. Paraffin sections were stained with antibodies to α-SMA as described in the Materials and Methods section. (**c**) The number of α-SMA-positive cells on the skin of uPAR$^{+/+}$ mice and uPAR$^{-/-}$ mice at the age of 18 weeks was determined at five randomly selected sites from different sections. The data represent the mean ± SEM. *$P<0.01$. (**d**) Type I collagen, type IV collagen, PAI-1, MMP-2, and MMP-9 gene expressions in the skin of uPAR$^{+/+}$ mice and uPAR$^{-/-}$ mice at the age of 18 weeks were determined by RT-PCR. The histogram on the right panels shows quantitative representations of the expression levels of the genes encoding type I collagen, type IV collagen, PAI-1, MMP-2, and MMP-9 obtained from densitometry analysis ($n=4$). The data are expressed as ratios of type I collagen, type IV collagen, PAI-1, MMP-2, and MMP-9 to GAPDH as percent increase relative to the skin of uPAR$^{+/+}$ mice. The data represent the mean ± SEM. *$P<0.01$. (**e**) The MMP activity was analyzed in skin from uPAR$^{+/+}$ mice and uPAR$^{-/-}$ mice by zymography at the age of 18weeks. The relative activity was quantified by scanning densitometry ($n=5$). The data represent the mean ± SEM. *$P<0.01$. Similar results were obtained with three additional and different skin samples.

alteration of fibrosis-related gene expression by uPAR deficiency, might therefore attenuate the degradation of ECM. Further investigation is thus required to clarify the details.

Recent studies have demonstrated that in scleroderma and other fibrotic diseases, reduced ECM turnover is a contributory factor for collagen accumulation and the development of dermal fibrosis (Arakawa *et al.*, 1996; Ghahary *et al.*, 1996; Hayashi *et al.*, 1996). MMPs are enzymes that can degrade most ECM proteins including collagen, which is the major protein component of fibrotic tissue (Matrisian, 1992; Parks, 1999). Plasmin directly activates proMMP-1, proMMP-3,

proMMP-9, proMMP-10, and proMMP-13 (Nagase *et al.*, 2006). The activation of proMMP-2 involves hydrolysis by MT1-MMP, yielding an intermediate that is activated by plasmin (Nagase *et al.*, 2006). In particular, both MMP-2 and MMP-9 cleave type IV collagen and several other ECM molecules (Nagase *et al.*, 2006). Therefore, the production and activity of MMP-2 and MMP-9 was investigated. These results indicate that the absence of uPAR attenuates the production and activity of MMP-2 and MMP-9. The activation of proMMP-9 may occur either through some plasmin-dependent mechanisms or through plasmin-independent mechanisms (Nagase *et al.*, 2006). uPAR might be involved in the production and activity of MMP-2 and MMP-9 regardless of the plasmin activity.

In conclusion, this study suggests that the absence of uPAR regulates fibrosis-related gene expression and MMP activity and also results in ECM deposition. As a result, the absence of uPAR induces dermal fibrosis. These findings may hopefully provide new insights into this field, which could eventually lead to the development of new clinical therapies for the prevention of fibrosis.

MATERIALS AND METHODS

Animals

Deficient mice were generated by homologous recombination using embryonic stem cells as described previously (Dewerchin *et al.*, 1996). All experiments were performed in accordance with institutional guidelines.

Reagents

All chemical substances were obtained from Sigma Chemical (St Louis, MO).

Skin distension ability in mice

Skin distension ability in the skin of male and female uPAR$^{+/+}$ mice and uPAR$^{-/-}$ mice at the age of 6, 10, and 18 weeks was measured using a Cutometer SEM474 suction extensometer ($n=6$). The section was applied to a 2 mm diameter area of the mouse's skin surface. The suction probe acted as a guard ring to preclude skin involvement outside of the area measured. The probe was fitted with a spring that ensured that it was applied to the skin at a constant pressure. Skin elongation was measured by an optical method with an accuracy of 0.01 mm using an infrared diode (Nishimori *et al.*, 2001).

Scanning electron microscopy

The back skin of male uPAR$^{+/+}$ mice and uPAR$^{-/-}$ mice at the age of 18 weeks was observed using an electron microscope S-3400N (Hitachi High-Technologies, Tokyo, Japan) ($n=3$). The samples were examined with the electron microscope at 15 kV.

Measurement of dermal thickness

The dermal thickness (distance from the epidermal–dermal junction to dermal–muscle junction) was measured in skin sections from male uPAR$^{+/+}$ mice and uPAR$^{-/-}$ mice at the age of 18 weeks ($n=7$).

Immunohistochemical staining of uPAR

The skin samples were obtained from male wild-type mice at the age of 6, 10, and 18 weeks. The skin samples were excised by using a punch biopsy instrument (Kai Medical, Gifu, Japan). Paraffin sections were labeled with anti-uPAR (rabbit IgG, Santa Cruz Biotechnology, Santa Cruz, CA) primary antibody and then secondarily labeled with FITC-conjugated anti-rabbit IgG (Invitrogen, Carlsbad, CA). The signals were then detected using a laser-scanning microscope. In each section, uPAR-positive cells were counted in four randomly chosen fields.

Collagen content in skin (the sircol biochemical assay)

The collagen content was measured as previously described (Kanno *et al.*, 2007). The collagen content was assessed using Sirius red staining. This approach was chosen because it accurately reflects the collagen content assessed with hydroxyproline assay and allows areas of localized collagen accumulation to be specifically evaluated. In these assays, sections of skin are stained with Sirius red as described by Junqueira *et al.* (1979). After deparaffinization, the skin sections are treated in 0.2% phosphomolybdic acid for 5 minutes. Next, the skin section was stained in 0.1% Sirius red for 90 minutes and in 0.01 N HCl for 2 minutes. The red stain was then detected using a laser-scanning microscope. In each section, Sirius red-positive area was measured in five randomly chosen fields and expressed as a percent of the observed in uPAR$^{+/+}$ mice.

Detection of myofibroblasts

Paraffin-embedded tissue sections from the skin were used to quantify the number of myofibroblasts by staining for α-SMA. After deparaffinization, the skin sections were immunostained with a mAb against α-SMA (clone 1A4; DakoCytomation, Glostrup, Denmark), according to the manufacturer's instructions, using the Dako Autostainer Universal Staining System. Thereafter, the sections were secondarily labeled with FITC-conjugated anti-rabbit IgG (Invitrogen). The signals were then detected using a laser-scanning microscope. In each section, α-SMA-positive cells were counted in five randomly chosen fields.

RT-PCR

RT-PCR was performed as previously described (Kanno *et al.*, 2006). Skin samples were obtained from male uPAR$^{+/+}$ and uPAR$^{-/-}$ mice at the age of 18 weeks. Total RNA was isolated from skin sample using Isogen (Nippon Gene, Tokyo, Japan) and was reverse-transcribed using M-MLV reverse transcriptase (Gibco BRL, Grand Island, NY). The transcripts were amplified by PCR using Ex Taq (TaKaRa, Kyoto, Japan). We used the following primer sequence: uPAR: 5′-TCCACCGAATGGCTTCCAGTG-3′ and 5′-AGACAACACGAGG GCACACAC-3′; PAI-1: 5′-AAAGGTATGATCAATGACTTACTGG-3′ and 5′-TCAAAGGGTGCAGCGATGAACATGC-3′; MMP-2: 5′-GAA CACCATCGAGACCATGC-3′ and 5′-CATCATGGATTCGAGAA AAG-3′; MMP-9: 5′-CAGCCGACTTTTGTGGTCTT-3′ and 5′-CGTG GTGTTCGAATGGCCTT-3′; type I collagen: 5′-ATCCCCATGACT GTCTATAG-3′ and 5′-CAAATAAGTGACCATCGCCA-3′; type IV collagen: 5′-TACCTGCCACTACTTCGCTAAC-3′ and 5′-CGGATGG TqGTGCTCTGGAAG-3′; GAPDH: 5′-TTCATTGACCTCAACTAC ATG-3′ and 5′-GTGGCAGTGATGGCATGGAC-3′. PCR amplification of cDNA for 35 cycles was included at 94 °C denaturation (60 seconds), 60 °C annealing (60 seconds), and 72 °C extension (60 seconds). After PCR amplification, the amplified cDNAs were further extended by additional incubation at 72 °C for 10 minutes. An equal amount of each reaction was separated by electrophoresis on 1% agarose gels and visualized with 10 mg/ml

EtBr, and the signal strengths were quantified using a densitometric program. After normalizing versus GAPDH intensity, percent increase was determined for each gene. Each experiment was repeated at least thrice.

Western blot analysis for uPAR

A western blot analysis was performed as previously described (Kanno *et al.*, 2008). Skin samples were obtained from male wild-type mice at the age of 6, 10, and 18 weeks. Samples were homogenized with lysis buffer (10 mM Tris-HCl, pH 6.8, containing 1% SDS and 1% Triton X-100) in the presence of proteases inhibitor cocktails (Sigma-Aldrich, St Louis, MO). The lysates were centrifuged at 15,000 r.p.m. for 10 minutes, and the resulting supernatants were collected. Proteins in the supernatant were separated by electrophoresis on 10% SDS-polyacrylamide gels and transferred to a nitrocellulose membrane. The membrane was incubated at 4 °C overnight with a polyclonal antibody to uPAR and then with peroxidase-conjugated antibody to rabbit IgG. Immunoreactive proteins were detected using ECL detection reagents (Amersham Pharmacia Biotech, Uppsala, Sweden). Each experiment was repeated at least thrice.

MMP activity assay

The MMP activity assay was determined utilizing gelatin substrate zymography. Skin samples were obtained from male uPAR$^{+/+}$ mice and uPAR$^{-/-}$ mice at the age of 18 weeks ($n=5$). Samples were mixed with SDS-loading buffer and incubated for 30 minutes at 37 °C. Samples and molecular weight markers were electrophoresed in a 10% polyacrylamide gel containing 0.1% gelatin. The gel was washed in 2.5% Triton X-100 to remove SDS and then incubated at 37 °C for 24–48 hours in 200 mM NaCl containing 40 mM Tris-HCl and 10 mM $CaCl_2$ (pH 7.5). After staining with Coomassie Blue R-250, gelatinases were identified as clear bands. The signal strengths were quantified using a densitometric program.

Statistical analysis

All data are expressed as the mean ± SEM. The statistical significance of the effect of each treatment ($P<0.01$) was determined by the analysis of variance (ANOVA) followed by the Student–Newman–Keuls test.

CONFLICT OF INTEREST

The authors state no conflict of interest.

REFERENCES

Arakawa M, Hatamochi A, Mori Y, Mori K, Ueki H, Moriguchi T (1996) Reduced collagenase gene expression in fibroblasts from hypertrophic scar tissue. *Br J Dermatol* 134:863–8

Bernstein AM, Twining SS, Warejcka DJ, Tall E, Masur SK (2007) Urokinase receptor cleavage: a crucial step in fibroblast-to-myofibroblast differentiation. *Mol Biol Cell* 18:2716–27

Blasi F, Carmeliet P (2002) uPAR: a versatile signalling orchestrator. *Nat Rev Mol Cell Biol* 3:932–43

D'Alessio S, Fibbi G, Cinelli M, Guiducci S, Del Rosso A, Margheri F *et al.* (2004) Matrix metalloproteinase 12-dependent cleavage of urokinase receptor in systemic sclerosis microvascular endothelial cells results in impaired angiogenesis. *Arthritis Rheum* 50:3275–85

Dewerchin M, Nuffelen AV, Wallays G, Bouche A, Moons L, Carmeliet P *et al.* (1996) Generation and characterization of urokinase receptor-deficient mice. *J Clin Invest* 97:870–8

Eitzman DT, McCoy RD, Zheng X, Fay WP, Shen T, Ginsburg D *et al.* (1996) Bleomycin-induced pulmonary fibrosis in transgenic mice that either lack or overexpress the murine plasminogen activator inhibitor-1 gene. *J Clin Invest* 97:232–7

Gabbiani G (2003) The myofibroblast in wound healing and fibrocontractive diseases. *J Pathol* 200:500–3

Ghahary A, Shen YJ, Nedelec B, Wang R, Scott PG, Tredget EE (1996) Collagenase production is lower in post-burn hypertrophic scar fibroblasts than in normal fibroblasts and is reduced by insulin-like growth factor-1. *J Invest Dermatol* 106:476–81

Hattori N, Degen JL, Sisson TH, Liu H, Moore BB, Pandrangi RG *et al.* (2000) Bleomycin-induced pulmonary fibrosis in fibrinogen-null mice. *J Clin Invest* 106:1341–50

Hayashi T, Stetler-Stevenson WG, Fleming MV, Fishback N, Koss MN, Liotta LA *et al.* (1996) Immunohistochemical study of metalloproteinases and their tissue inhibitors in the lungs of patients with diffuse alveolar damage and idiopathic pulmonary fibrosis. *Am J Pathol* 149:1241–56

Highland KB, Silver RM (2005) New developments in scleroderma interstitial lung disease. *Curr Opin Rheumatol* 17:737–45

Junqueira LC, Bignolas G, Brentani RR (1979) Picrosirius staining plus polarization microscopy, a specific method for collagen detection in tissue sections. *Histochem J* 11:447–55

Kanno Y, Hirade K, Ishisaki A, Nakajima K, Suga H, Into T *et al.* (2006) Lack of alpha2-antiplasmin improves cutaneous wound healing via over-released vascular endothelial growth factor-induced angiogenesis in wound lesions. *J Thromb Haemost* 4:1602–10

Kanno Y, Into T, Lowenstein CJ, Matsushita K (2008) Nitric oxide regulates vascular calcification by interfering with TGF-beta signalling. *Cardiovasc Res* 77:221–30

Kanno Y, Kuroki A, Okada K, Tomogane K, Ueshima S, Matsuo O *et al.* (2007) Alpha2-antiplasmin is involved in the production of transforming growth factor beta1 and fibrosis. *J Thromb Haemost* 5:2266–73

Knapp TR, Daniels RJ, Kaplan EN (1977) Pathologic scar formation. Morphologic and biochemical correlates. *Am J Pathol* 86:47–69

Loskutoff DJ, Quigley JP (2000) PAI-1, fibrosis, and the elusive provisional fibrin matrix. *J Clin Invest* 106:1441–3

Ludwicka A, Trojanowska M, Smith EA, Baumann M, Strange C, Korn JH *et al.* (1992) Growth and characterization of fibroblasts obtained from bronchoalveolar lavage of patients with scleroderma. *J Rheumatol* 19:1716–23

Margheri F, Manetti M, Serrati S, Nosi D, Pucci M, Matucci-Cerinic M *et al.* (2006) Domain 1 of the urokinase-type plasminogen activator receptor is required for its morphologic and functional, beta2 integrin-mediated connection with actin cytoskeleton in human microvascular endothelial cells: failure of association in systemic sclerosis endothelial cells. *Arthritis Rheum* 54:3926–38

Matrisian LM (1992) The matrix-degrading metalloproteinases. *Bioessays* 14:455–63

Mondino A, Resnati M, Blasi F (1999) Structure and function of the urokinase receptor. *Thromb Haemost* 82:19–22

Nagase H, Visse R, Murphy G (2006) Structure and function of matrix metalloproteinases and TIMPs. *Cardiovasc Res* 69:562–73

Nishimori Y, Edwards C, Pearse A, Matsumoto K, Kawai M, Marks R (2001) Degenerative alterations of dermal collagen fiber bundles in photo-damaged human skin and UV-irradiated hairless mouse skin: possible effect on decreasing skin mechanical properties and appearance of wrinkles. *J Invest Dermatol* 117:1458–63

Parks WC (1999) Matrix metalloproteinases in repair. *Wound Repair Regen* 7:423–32

Sappino AP, Schurch W, Gabbiani G (1990) Differentiation repertoire of fibroblastic cells: expression of cytoskeletal proteins as marker of phenotypic modulations. *Lab Invest* 63:144–61

Hunt TK (1990) Basic principles of wound healing. *J Trauma-Injury Infect Crit Care* 30:S122–8

Zhang G, Kim H, Cai X, López-Guisa JM, Alpers CE, Liu Y *et al.* (2003) Urokinase receptor deficiency accelerates renal fibrosis in obstructive nephropathy. *J Am Soc Nephrol* 14:1254–71